Supplementary material

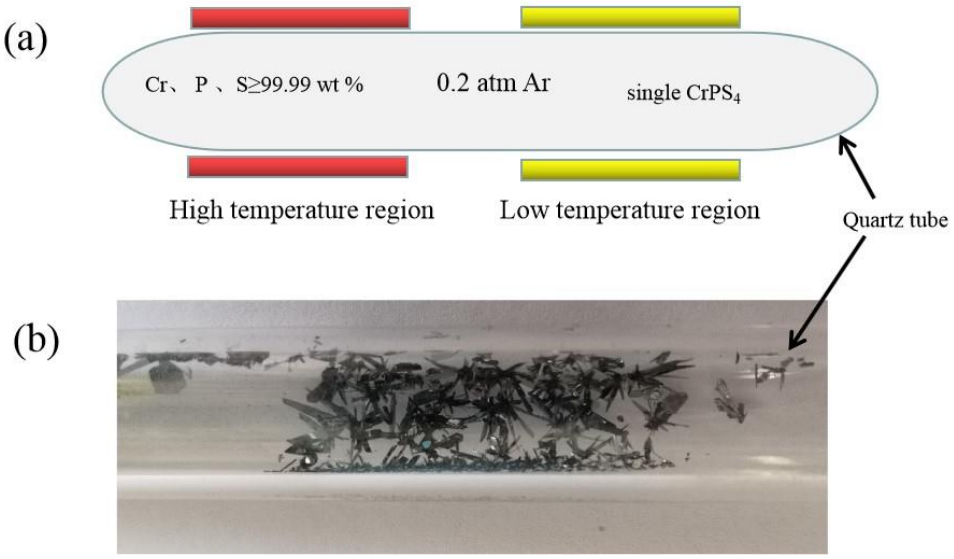

FIG.S1. (a) Schematic illustration of CVT (chemical vapor transport) growth of $CrPS_4$ crystals from raw materials in a vacuum-sealed ampoule. (b) CVT growing sample of $CrPS_4$ crystals.

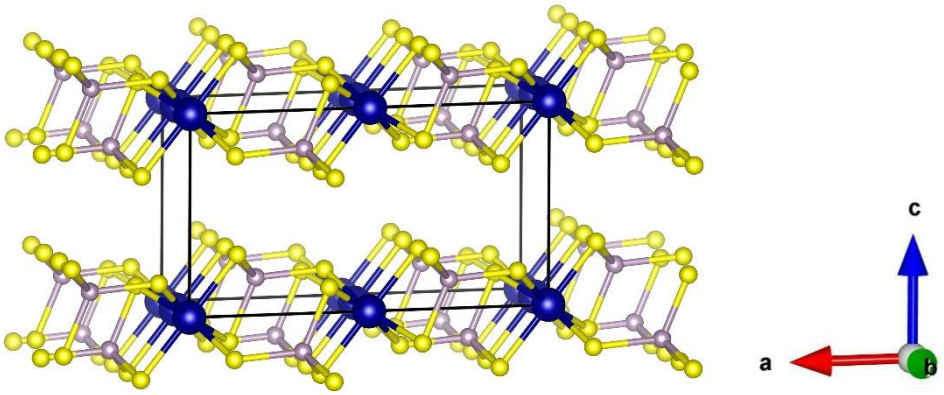

FIG.S2. Crystal lattice structure and exfoliated sample of $CrPS_4$.

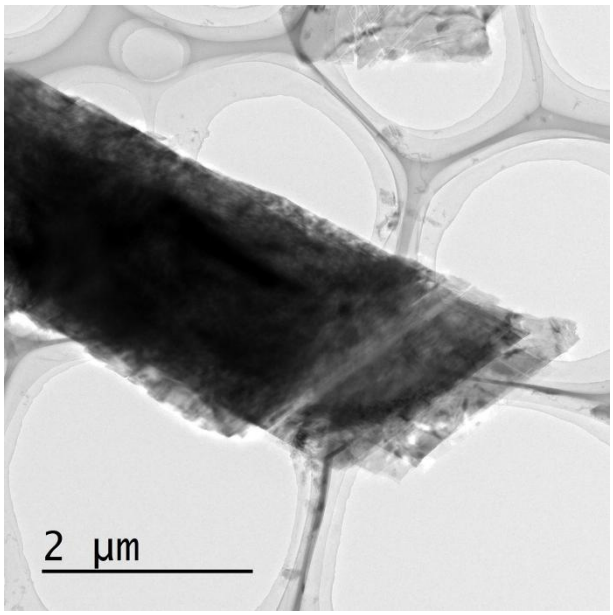

FIG.S3. TEM image of the exfoliated $CrPS_4$ samples .

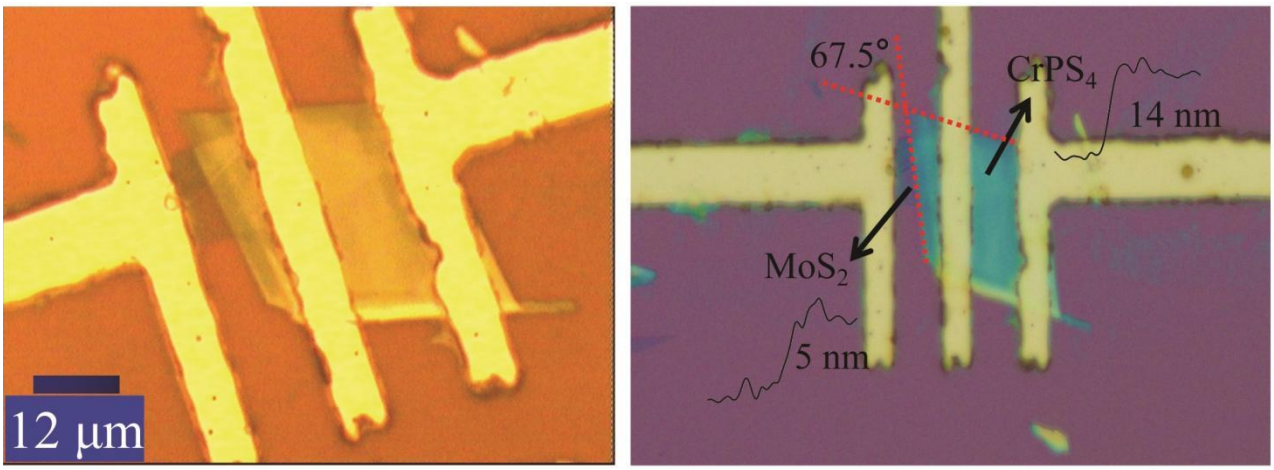

FIG.S4. Schematic diagram of the structure for the back gate MS-CPS photodetector together with electrical connections to characterize the device.

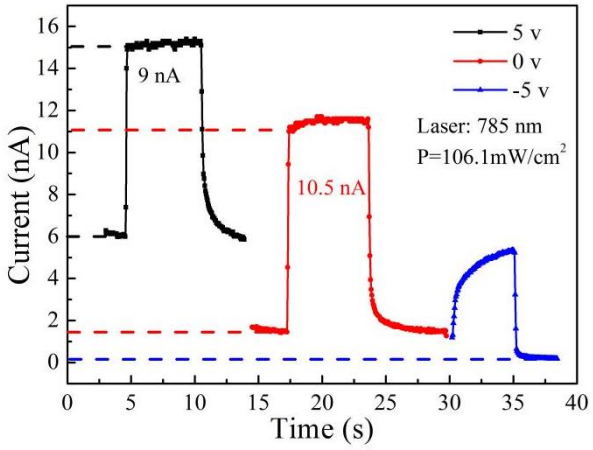

FIG.S5. temporal interlayer photoresponse curves for the MS-CPS photodetector under positive, zero, and negative gate voltages at 785 wavelength.

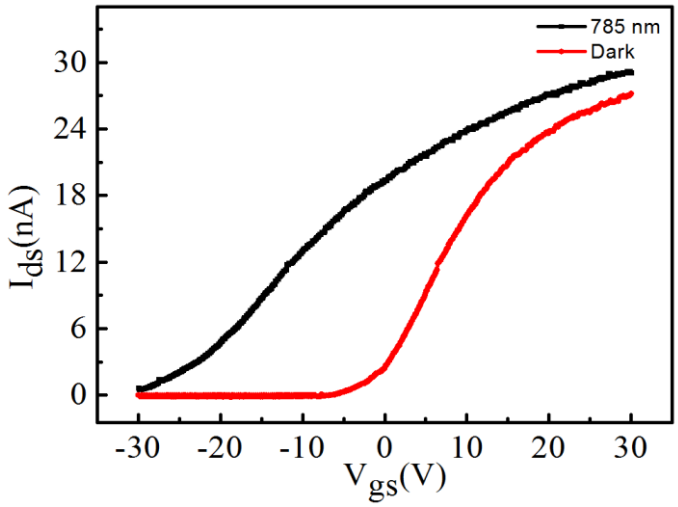

FIG.S6. I_{drain}–V_{gate} characteristics of the MS-CPS photodetector under dark (black line) and illuminated (red line) conditions (λ = 785 nm).

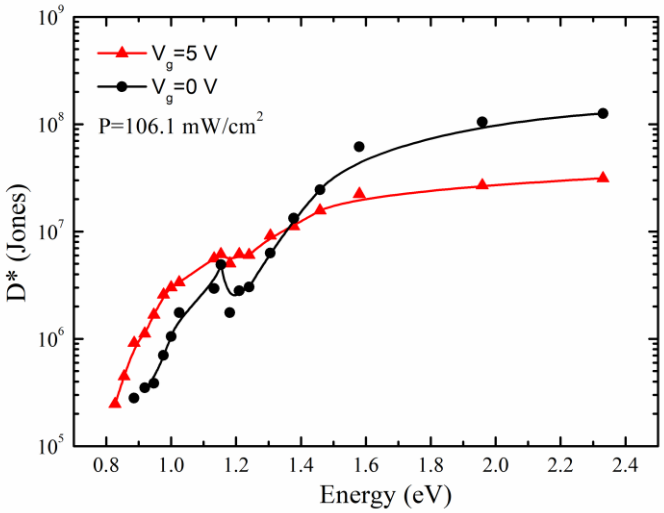

FIG.S7. Wavelength dependence of D* from 532 to 1500 nm for the photodetectors with the illumination power intensity of 106.1 mW/cm^2

D* can be expressed as :

$$D^* = \frac{\sqrt{A\Delta f}}{NEP}$$

where A is the photosensitive area, Δf is the electrical bandwidth, and NEP is the noise equivalent power of the device at the same measuring condition.

measuring condition.

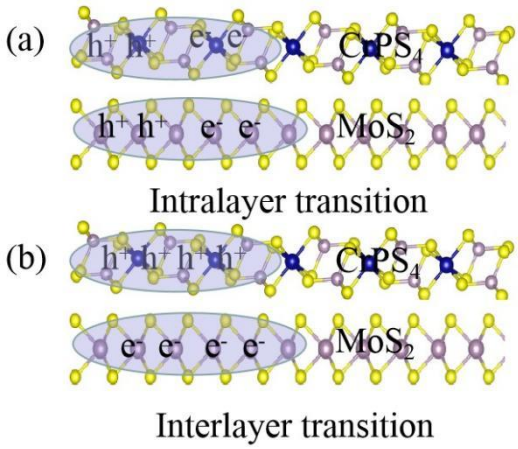

FIG.S8. Spatially separation of the intralayer excitons and interlayer excitons.

Table S1. The performance summary of for relevant heterostructures for infrared photodetectors.

Material	Bias voltage	Wavelength	Detectivity	Photo current(pA)	Reference
WS_2/MoS_2	-1=V	1030 nm	Not provided	3 pA	Wang et al[9]
WSe_2/ReS_2	-0.5=V	1250 nm	Not provided	20 pA	Varghese et al[17]
graphene/MoS_2/Au	1=V	785 nm	10^7 Jones	300 pA	Liu et al[22]
GaTe/InSe	1=V	1550 nm	10^{12} Jones	10 pA	Tailei Qi et al[42]
$CrPS_4/MoS_2$	2=V	785	6.16×10^7 Jones	7 nA	This work
	2=V	1350	1.1×10^6 Jones	400 pA	

9 Wang, G. C.; Li, L.; Fan, W. H.; Wang, R. Y.; Zhou, S. S.; Lü, J. T.; Gan, L.; Zhai, T. Y. Interlayer Coupling Induced Infrared Response in WS_2/MoS_2 Heterostructures Enhanced by Surface Plasmon Resonance. Adv. Funct. Mater. 2018, 1800339.

17 Abin Varghese.; Dipankar Saha, Kartikey Thakar.; Vishwas Jindal.; Sayantan Ghosh.; Nikhil V Medhekar.;Sandip Ghosh.; Saurabh Lodha. Near-Direct Bandgap WSe_2/ReS_2 Type-II pn Heterojunction for Enhanced Ultrafast Photodetection and High-Performance Photovoltaics. Nano Lett. 2020, 20, 1707-1717.

22 Liu, B., Chen, Y., You, C., Liu, Y., Kong, X., Li, J., ... & Zhang, Y. (2019). High performance photodetector based on graphene/MoS2/graphene lateral heterostrurcture with Schottky junctions. Journal of Alloys and Compounds, 779, 140-146.

42 Qi, T. L.; Gong, Y. P.; Li, A. L.; et al. Interlayer Transition in a vdW Heterostructure toward Ultrahigh Detectivity Shortwave Infrared Photodetectors. Adv. Funct. Mater. 2020, 30, 1905687.